Development of the Exowave Oscillating Wave Surge Converter

Sarah K. Iversen, Jacob Andersen, and Peter Frigaard

Abstract—**With increasing demand for renewable energy resources, the development of alternative concepts is still ongoing. The wave energy sector is still in vast development on the way to contribute to the energy production world wide. The present study presents the development of the Exowave wave energy converter made so far. A numerical model has been established supported by wave flume tests performed at Aalborg University during the first phase of the development. Furthermore, a successful open sea demonstration has been performed on 7 meters of water at Blue Accelerator, Belgium, from which the concept has been proven. As part of the ongoing research, verification of the numerical model will be made through experimental testing in the wave tank of Aalborg University, and an open sea demonstration at 14 meters of water depth will be executed off the coast of Hanstholm, Denmark.**

Index Terms—**Wave energy, WEC, Morison equation, numerical modelling, wave flume tests.**

I. Introduction

THE political push towards renewable energy sources along with strategies to mitigate audible and visual pollution have encouraged offshore deployment of renewable energy devices such as wave energy converters (WECs) which if integrated with offshore windfarms can increase utilization of otherwise dedicated marine spaces and critical infrastructure, i.e., substations, transformers, grid, etc. Exowave is a wave energy converter of the oscillating wave surge type with a bottom-hinged wave-activated body that moves in pitch when excited by waves. Of other wave energy converters of the oscillating wave surge type, Oyster [1], or WaveRoller [2] can be mentioned. Common for these two devices is the flap-like shape of the wave-activated body. In both cases, the flap covers more or less the entire water column from seabed to water surface, and with a width/height ratio larger than 1. For the Exowave device, the original idea was to create a smaller device, with a flap arm connecting the flap in the upper part of the water column with the hinge at the foundation and place the devices in clusters The Exowave WEC is a multifunctional device, that can produce fresh water or electricity as needed. As other WECs of this type, the concept is a fully submerged solution to secure survivability during extreme events, which is known to be a challenge for many other wave energy devices. Furthermore, audible and visual pollution is avoided, when the device is fully submerged. The aim for the implementation of Exowave is a better utilization of dedicated offshore wind energy areas, as it can be integrated in offshore wind farms and connected to critical infrastructure, i.e. substations, transformers, grid, etc. The WEC consists of a gravity-based foundation. Attached to the foundation is a bottom-hinged power-take-off (PTO), which is driven by a buoy-like wave-activated body, which is connected to the PTO. Through a flow line pipe system, the PTO is connected to a water turbine electrical generator.

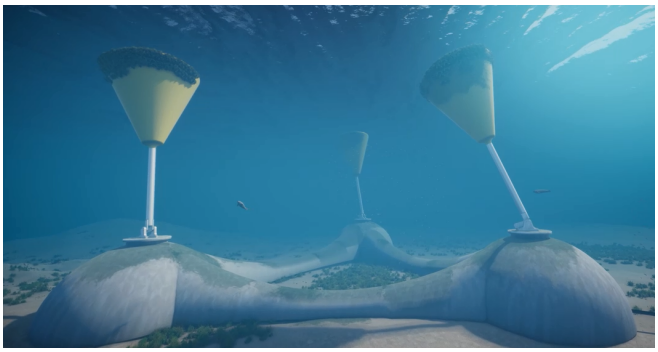

Fig. 1. Exowave Cluster

For estimation of power production and structural design of wave energy converters, numerical modelling is key. The development of a numerical model is highly dependent on the design and size of the wave-activated body in proportion to the sea state at the target location of the device, as the model must be able to capture the relevant phenomena associated with the specific wave regime as given by [3]. This paper will therefore present the development of the Exowave wave energy converter as seen in Fig. 1, with focus on the design of the wave-activated body and numerical modelling of the movement hereof including power production. An overview of research performed so far will be given, which has lead to the current design of the device. Additionally, the plans for the ongoing and future development will be presented.

II. Research performed until now

The development of Exowave kickstarted with the project *Exowave, Water, Electricity and PtX* which was supported by The Danish Energy Agency under The Energy Technology Development and Demonstration

This work was supported by The Danish Energy Agency under The Energy Technology Development and Demonstration Program (EUDP) contract number 64022-1062, Niels Bohrs Vej 8D, 6700 Esbjerg, Denmark.

S. K. Iversen (e-mail: ski@build.aau.dk), J. Andersen and P. Frigaard is with the Department of the Built Environment at Aalborg Universitet, Thomas Manns Vej 23, 9220 Aalborg Øst, Denmark.

Digital Object Identifier:
https://doi.org/10.36688/ewtec-2023-368

Program, wherefore it will in the following be referred to as EUDP1. The objective of EUDP1 was to develop a numerical model for estimation of power production and for use in structural design of the device, to investigate the feasibility and business case for a combined wave energy and offshore wind plant, to perform wave tank testing and CFD analysis, and lastly to demonstrate the device in open water for verification of the numerical model. The following sections will present the outcomes of EUDP1 performed by Aalborg University, which relates to the design of the wave-activated body and the numerical modelling and wave flume testing hereof.

III. Numerical model

For estimation of the power production and for use in the structural design of the device, a numerical model for the interaction between the wave loads and the wave-activated body has been developed by Aalborg University. The numerical model is described in the following. Based on the wave force regime by Chakrabarti [3], the numerical model is designed to include the inertia and drag effects. The numerical model for the Exowave converter is therefore based on the Morison equation [4], which is applicable in the inertia and drag dominated wave force regimes. It is therefore assumed that there are no diffraction effects. The wave kinematics used in the numerical model are evaluated using linear wave theory for regular or irregular waves.

For structural design of the device as well as estimation of the energy production, the loads involved in movement of the wave-activated body must first be defined. The wave forces are calculated from the Morison equation as given by [4], as it is assumed that the characteristic length of the WEC is small relative to the characteristic wavelengths of the target wave climates. For a moving body, the Morison force is calculated using (1). The resulting wave force and moment at the point of rotation are calculated using Simpson integration.

$$\begin{aligned} f_\perp(t) =& \rho A \frac{du}{dt} + \rho C_A A \left(\frac{du_\perp}{dt} - \ddot{\theta} r \right) \\ &+ \frac{1}{2} \rho C_D D \left(u_\perp - \dot{\theta} r \right)^2 sgn \left(u_\perp - \dot{\theta} r \right) \end{aligned} \tag{1}$$

where

ρ	Density of water, [kg/m^3]
A, D	Characteristic cross area and length normal to flow direction [m^2, m]
u	Horizontal wave particle velocity, [m/s]
$u_\perp$	Wave particle velocity orthogonal to body [m/s]
C_A, C_D	Added mass and drag coefficients, [-]
$\dot{\theta}, \ddot{\theta}$	Angular velocity and acceleration of body [rad/s, rad/s^2]
r	Distance from hinge to point on body [m]

The hydrostatic forces on the energy-collector are the buoyancy and the gravity, which work in opposite directions, wherefore the hydrostatic moment at the point of rotation is expressed from (2).

$$\begin{aligned} M_{hydro} &= M_{buo} - M_{gravity} \\ &= \rho g V \sin(\theta) r_b - mg \sin(\theta) r_m \end{aligned} \tag{2}$$

where

g	Gravitational acceleration, [m/s^2]
V	Volume of energy-collector, [m^3]
r_b	Distance from hinge to centre of buoyancy, [m]
m	Mass of energy-collector, [kg]
r_m	Distance from hinge to centre of gravity, [m]

The power take-off (PTO) consists of a double acting hydraulic system with a pressure p_{hydr}. The PTO is activated when $\theta > 0 \wedge \dot{\theta} > 0$ or $\theta < 0 \wedge \dot{\theta} < 0$. The reacting force from the PTO piston is $F_{piston} = p_{hydr} A_{hydr}$, where A_{hydr} is the effective internal area of the hydraulic cylinder. The moment at the point of rotation due to the PTO is then calculated from (3) with respect to the arm, d, which is calculated from trigonometry as a function of θ.

$$M_{PTO} = F_{piston} d(\theta) \tag{3}$$

The WEC is modelled as a one degree-of-freedom (DoF) system, which is free to move in pitch, when it is excited by waves. The dynamic system is described from the equation of motion as stated in (4), where K is the rotational stiffness, C is the rotational damping coefficient, I is the moment of inertia and M_{res} is the resulting moment of the system as specified in (5).

$$K\theta(t) + C\dot{\theta}(t) + I\ddot{\theta}(t) = M_{res}(\theta, \dot{\theta}, \ddot{\theta}) \tag{4}$$

The resulting moment consists of the resulting Morison moment, M_{mor}, the hydrostatic moment, $M_{hydrostat}$, and the PTO moment, M_{PTO}:

$$\begin{aligned} M_{res}(\theta, \dot{\theta}, \ddot{\theta}) =& M_{mor}(\theta, \dot{\theta}, \ddot{\theta}) + M_{hydrostat}(\theta) \\ &+ M_{PTO}(\theta, \dot{\theta}) \end{aligned} \tag{5}$$

The equation of motion is then represented in state space as two ordinary differential equations. When the PTO is active, the system is considered highly nonlinear, wherefore it is solved using a Runge-Kutta solver following the implementation by [5] and [6].

IV. Development of WEC Design

During the numerical modelling with regard to the target wave climate at the future position of the WEC, simulations showed that the system was more inertia dominated than drag dominated, wherefore the design of the wave-activated body was lead to an idea of a more cylindrical shape. The shape was therefore changed from the initial idea of having a flat flap-like shape to being frustum of a cone to reduce the drag coefficient, as the drag will damp the movement of the system. Furthermore, the idea of the conical design was to increase the width at the top of the body to match the velocity profile of the water particles.

A first estimate of the inertia and drag coefficients was therefore based on literature review. The estimations are based on the recommendations from [7]. For two-dimensional bodies, the added mass coefficient of a cylinder in infinite fluid is 1.0. As a two-dimensional body, no effects from the free surface or other 3-dimensional effects are taken into account. Intuitively, this implies that the added mass coefficient of the system might be below 1.0, when the 3D effects are considered. For a fixed cylinder in a steady flow with Reynolds number of approximately 10^5, the drag coefficient is in the range of 0.5-1.0 depending on the roughness of the surface. The determination of added mass and drag coefficients for a cone-like structure for a given wave climate is however associated with large uncertainties, wherefore experimental testing in the wave flume were performed to support the choice of coefficients in the numerical model.

V. Wave flume tests

This section will describe the wave flume tests performed in the flume at the Ocean and Coastal Laboratory at Aalborg University as part of EUDP1. The test included different float model designs and the determination of Morison coefficients hereof. The outcome of the two tests is given in the following.

A. Morison Coefficients

The test setup for the flume tests conducted at Aalborg University was based on a potential design for a 100kW rated power WEC cell to be deployed at the site Thor off the coast of Hvide Sande, Denmark. The scope of the model tests were to calculate Morison coefficients for different shapes of the wave-activated body for various sea states defined based on the Keulegan-Carpenter (K_C) number, and secondly to assess the influence of the geometry of the body on the wave loading. Test specimens were delivered by Exowave Aps. The different designs tested are illustrated in Fig. 2 The tests were performed in the wave flume with a horizontal bed and water depth of 0.645m, corresponding to 25.8m in prototype scale. The test setup in the flume appears from Fig. 3. Force transducers to measure loads in the wave propagation direction were installed at the top of the model as illustrated in Fig. 3. All tests were repeated with no model floats but instead a wave gauge installed at the model float location. Identical steering signals for wave generation were applied between repeated sea states. The force transducers and wave gauge signals were logged utilizing WaveLab 3.858 [8]. The different designs were all tested for target sea states of which the K_C-numbers were kept constant for all three designs. The K_C numbers were calculated from:

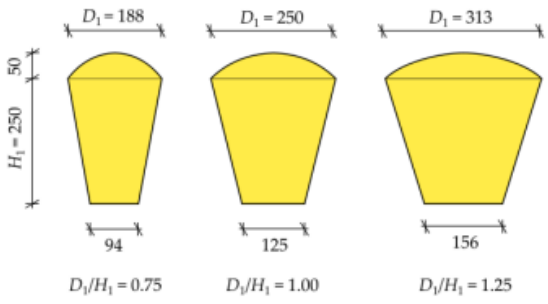

Fig. 2. Dimensions of investigated float model designs (axisymmetric) [mm]

$$K_C = \frac{u_{max,0} T}{D_{av}} \tag{6}$$

where $u_{max,0}$ is the horizontal maximum particle velocity at SWL [m/s], T is the wave period [s], and D_{av} is the average of D_1 and the bottom diameter [m]. $u_{max,0}$ was calculated from stream function theory, i.e., specifically from the Fourier approximation method by [9]. Only regular sea states were investigated. The waves were generated from second order theory as per [10] with modifications by [11] for K_C of max. 3 or from approximate stream function theory as per [12] for larger K_C numbers.

For calculation of the wave loads, the Morison equation was applied, which models the wave force on a structure as a linear combination of inertia and drag loads. For the static float, the horizontal force per unit length, f [N], is expressed from the Morison equation in (1), here with the velocity of the body being equal to 0.

The resulting force F_x was calculated by integrating f over the height of the float. The Morison coefficients, $C_M = C_A + 1$ and C_D, were calculated by a least squares approach adopted from [13]. For inertia dominated regimes, the experimental determination of the drag coefficient is associated with very high sensitivity, wherefore $C_D = 0.8$ was imposed as found from numerical tests with computatioanl fluid dynamics (CFD), see Section V-B.

B. Calculation of Drag Coefficient from CFD

Numerical tests with CFD were carried out by Delft University and Aalborg University to calculate the drag coefficient for a fixed float model with the top point tangential to the still water level. The open-source, cell-centred finite volume CFD framework of OpenFOAM [14] was used to set up a three-dimensional, two-phase (water and air) model with uniform inflow velocity of 0.5 m/s ($Re \approx 1e5$). The grid was structured with predominantly hexahedrals and wall functions were employed at the no-slip boundaries of the float model. A domain size of 5 float diameters upstream of the model, 15 float diameters downstream, and about 3 diameters to either side patch was used. The interFoam solver of OpenFOAM-v2012 (ESI) was employed to numerically solve the Reynolds-Averaged Navier-Stokes equations with turbulence closure from the k-omega-SST model as per [15] Time stepping was done by a maximum Courant criterion of 0.1. The fluid-structure interaction problem yielded $C_D = 0.8$ after development of a steady state.

C. Results

The measured wave height and wave periods are used to calculate five time series of the resultant F_x.

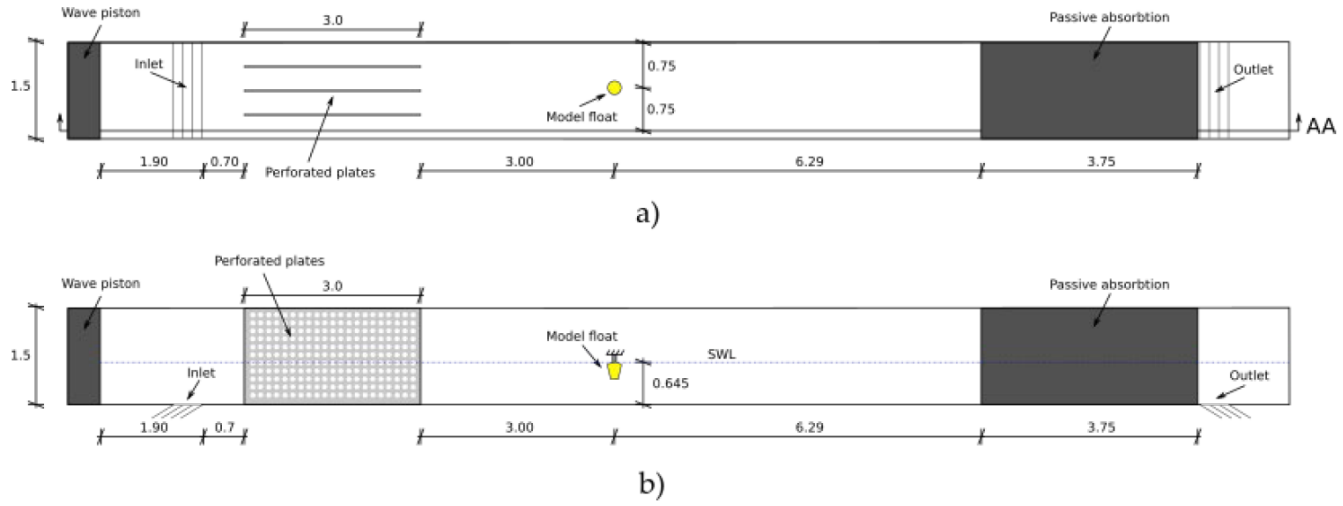

Fig. 3. Setup of the flume, a) top view, b) Section view A-A. [m]

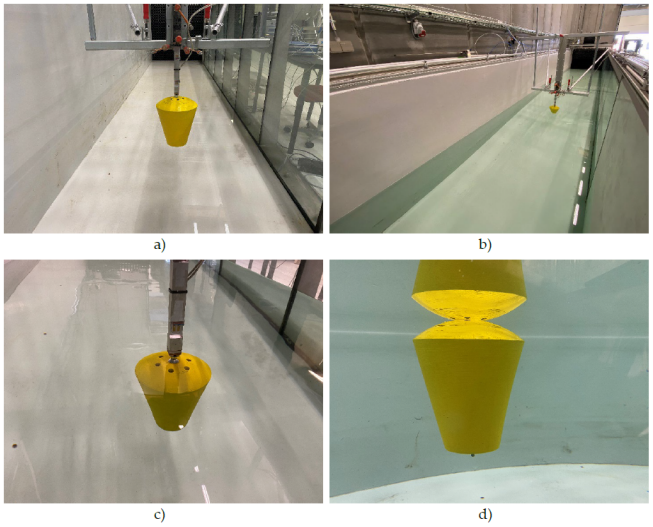

Fig. 4. Photos of the test setups: a) Installed model float with no water in flume, b) Installed float model with water, passive absorption in the background, c) Force transducer mounted on top of float model, d) SWL and top of float model coinciding.

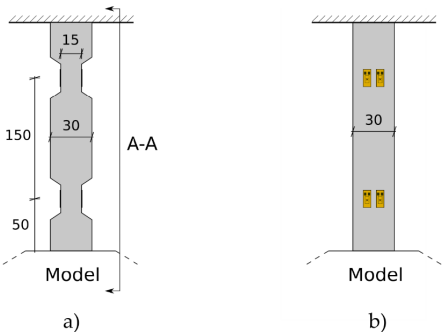

Fig. 5. Force transducer mounted on top of the float models [mm]. a) Transverse of the wave propagation direction view, b) Section A-A view.

The measured surface elevation time series and the measured force time series were aligned from adjacent zero-down-crossings from the surface elevation time series. The least squares error approach is utilized to estimate the Morison coefficients for each of the

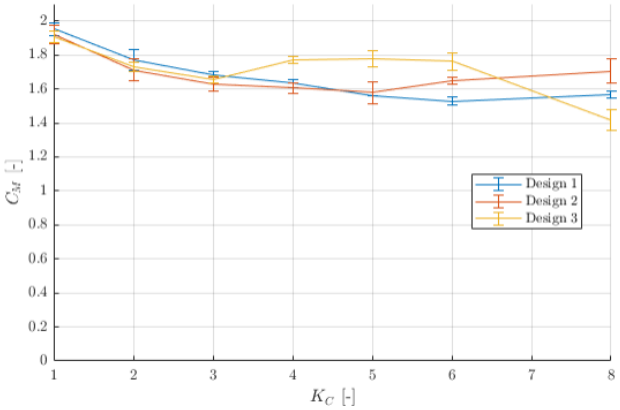

Fig. 6. Mean inertia coefficients, $C_M = 1 + C_A$, as function of investigated KC numbers. Error bars of plus/minus 2 standard deviations are included.

calculated resultant time series (5 repetitions) with each of the measured force time series (5 repetitions). Thus, a total of 25 sets of Morison coefficients is calculated for each sea state. Fig. 6 illustrates the average inertia coefficient, $C_M = 1 + C_A$, with plus/minus two standard deviations for each sea state (K_C) for all three designs. For all designs, the inertia coefficients are seen to depend significantly on the K_C number. E.g. a decrease from approximately $C_M = 1.9$ at $K_C = 1$ to approximately $C_M = 1.6$ at $K_C = 3$ is present for all designs. From [16], the inertia coefficient of a 2D-cylinder for $K_C < 4 (Re \approx 2 \cdot 10^4)$ is 2.0 (from U-tube experiments). Intuitively, 3D effects of flow under and over a cylindrical structure will mitigate wave loads relative to a 2D cylinder, in compliance with the C_M values in Fig. 6. An increase in C_M occurs for all three designs for K_C values corresponding to a wavelength of around 4.8m, i.e. $K_C = 8$ for Design 1, $K_C = 6$ for Design 2, and $K_C = 4$ for Design 3. Reflective wave loads will be more dominant for longer waves, as these waves will have ramped further up when re-impacting the float model than for shorter waves. The aforementioned increases of C_M are ascribed to reflective wave effects, and considering C_M of the shorter wavelengths

in suggests that C_M will equal 1.5-1.6 for the highest investigated K_C numbers. No significant differences between inertia coefficients of the different designs are present for K_C corresponding to wavelengths less than 4.8m. Variations between trials were present for most tested sea states. These are ascribed to inaccuracies in the trigger signal system, and could in further analyses be mitigated from cross-correlation analysis of both surface elevation and force signals.

D. Conclusions

Inertia coefficients are determined for seven different K_C numbers for three different designs. The inertia coefficients strongly depend on the K_C numbers, and ranges from approximately 1.9 for $K_C = 1$ to approximately 1.5-1.6 for $K_C = 6$. Calculated inertia coefficients for K_C numbers corresponding to longer wavelengths are more subjected to reflective wave loads in the wave flume. For wavelengths larger than 4.8m in the present tests, inertia coefficients are expected to be overestimated. No significant differences of the inertia coefficients are found between designs for wavelengths shorter than 4.8m. Thus, Design 3 will yield the largest amplitude of a wave load cycle, since the cross-sectional area of this design is larger than for Design 1 and 2.

VI. Open Sea Demonstration

The EUDP1 project terminated with an open sea demonstration of the WEC10 converter. The demonstration was performed at Blue Accelerator, Belgium. The location provided a water depth of 7 meters with 4-5m tidal deviations and a 1m/s tidal current, which is rather different from the future intended location of the Exowave converter. The demonstration provided a proof of the installation principles for future use. The foundation was assembled on land. The PTO was installed in the foundation, and the wave-activated body was installed on top. The WEC10 can be seen in Fig. 7 before launch. Furthermore, a ballast test was performed as seen in Fig. 8, before the WEC was successfully towed to the desired location at sea as shown in Fig. 9, where it was ballasted with seawater and placed on the sea bed. The WEC was calibrated to start production at 45 bar counter pressure, which should be possible at a sea state with a significant wave height of 1m. The production during the demonstration was measured as the flow produced by the hydraulic piston. The data acquisition took place during September and October 2022. Due to a very mild climate during the data acquisition period, the recorded data was mainly useful for proof of the concept. More data will be necessary for further verification of the numerical model. After demonstration, the device was successfully uninstalled and transported back to the workshop, where it will be used for further analysis of the components.

VII. Conclusion

The research performed so far at Aalborg University of the Exowave wave energy converter has lead to a conical design of the wave-activated body. The idea behind the axisymmetric body is to reduce the drag, as the drag will damp the movement of the body. This design is different to other wave energy converters developed so far. A numerical model is developed based on present design, from which the structural design of the device and power production hereof can be estimated. The numerical model is based on the Morison equation, as the characteristic length of the Exowave is small relative to the characteristic wavelengths of

Fig. 7. WEC10 prepared for launch at Blue Accelerator, Belgium.

Fig. 8. Ballast test, Blue Accelerator, Belgium.

Fig. 9. Towing of WEC to site, Blue Accelerator, Belgium.

the target wave climates. The Morison coefficients used in the formulation of the numerical model have been calculated from physical wave flume test performed in the wave flume at the Ocean and Coastal Laboratory at Aalborg University, and by numerical tests from two-phase CFD analyses. The current design of the wave energy device has been demonstrated in open sea at Blue Accelerator, Belgium, from which the installation principles and conceptual design are found successful.

VIII. Future development

The future development is already in process with a new project supported by The Danish Energy Agency under The Energy Technology Development and Demonstration Program as well, therefore referred to in the following as EUDP2. The objectives of the EUDP2 project is to verify the numerical model for demonstration at 14 m water depth in the North Sea for a cell power of 35kW (WEC35), to implement yaw control of the device, to optimize the flap shape and to balance the system pressure to improve the capacity factor. Another degree of freedom is added to the WEC system to reduce the loads in the direction perpendicular to the mean direction of wave propagation, wherefore the system will be free to move in roll. The power production will still be for the movement in pitch. The numerical model and demonstration from the EUDP1 project did not cover this movement, wherefore additional wave tank tests will be performed at Aalborg University, before the demonstration at open sea will take place.

A. Wave tank tests

New wave tank tests performed at Aalborg University aims to test a moving system of the WEC35. An active PTO will be added to the small scale model to verify the power production estimated from the numerical model. Furthermore, the behavior of the system that is free to move in roll will be investigated for multidirectional waves. The study will furthermore investigate the loss of efficiency due to multidirectionality of the waves. Where the designs in the wave flume tests presented in this paper primarily focused on different sizes of the conical body, the coming tests will furthermore focus on the influence of different shapes, to see if any significant difference is experienced for the new system. The tests will consider the amplitude of the response as well and the band-width hereof.

B. Demonstration North Sea

For EUDP2 a open sea demonstration at 14 m water depth is planned. The demonstration will take place at the Danish Wave Energy Centre (DanWEC) off the coast of Hanstholm, Denmark, in the North Sea. The aim of the demonstration is to verify the energy production. The hydraulic system of the PTO will be connected to a water turbine generator onshore. Performance wise, the demonstration aims to implement yaw control of the device in order to orientate the device according to the measured mean wave direction on the site. Furthermore an active control system of the hydraulic PTO system is expected to be implemented. For verification of the numerical model in relation to power production and structural design, the motion of the wave-activated body will be monitored as well as the loads, which will be monitored by strain gauges on the arm connecting the body to the PTO and foundation. The demonstration furthermore seeks to prove a new installation procedure for a concrete foundation in stead of the steel foundation used for the demonstration in EUDP1. Of other materials, it is considered using glass fibres from wind turbine blade waste material to produce the wave-activated body.

Acknowledgement

References

[1] T. Whittaker, D. Collier, M. Folley, M. Osterried, A. Henry, and M. Crowley, "The development of oyster — a shallow water surging wave energy converter." *Proceedings of the 7th European wave and tidal energy conference*, 2007.
[2] AW Energy. (2022) Waveroller. Accessed: 2023-05-22. [Online]. Available: http://https://aw-energy.com/
[3] S. K. Chakrabarti, *Hydrodynamics of Offshore Structures*. Springer Verlag, 1987.
[4] J. R. Morison, M. P. O'Brien, J. W. Johnson, and S. A. Schaaf, "The forces exerted by surface waves on piles," *Petroleum Transactions*, vol. 189(5), pp. 149–154, 1950.
[5] J. R. Cash and A. H. Karp, "A variable order runge-kutta method for initial-value problems with rapidly varying right-hand sides," *ACM Transactions on Mathematical Software*, vol. vol. 16, pp. 201–222, 1990.
[6] H. P. Gavin, *Numerical Integration in Structural Dynamics*. Department of Civil & Environmental Engineering, Duke University, 2020.
[7] Det Norske Veritas, "DNV-RP-C205: Environmental conditions and environmental loads," DNV A/S, Recommended Practice, Sep. 2019.
[8] P. Frigaard and T. L. Andersen, *Analysis of Waves: Technical Documentation for WaveLab 3*. Department of Civil Engineering, Aalborg University; ISSN:1901-7286, 2014.
[9] M. M. Rienecker and J. D. Fenton, "A Fourier approximation for steady water waves," *J. Fluid Mech.*, vol. 104, 1981.
[10] H. A. Schäffer, "Second-order wavemaker theory for irregular waves," *Ocean Engineering*, vol. 23, pp. 47–88, 1996.
[11] M. R. Eldrup and T. L. Andersen, "Applicability of nonlinear wavemaker theory," *J. Mar. Sci. Eng.*, vol. 7, 2019.
[12] H. Zhang and H. A. Schäffer, "Approximate stream function wavemaker theory for highly nonlinear waves in wave flumes," *Ocean Engineering*, vol. 34, pp. 1290–1302, 2007.
[13] H. F. Burcharth, *Strøm- og Bølgekræfter på Stive Legemer*. Aalborg University, 2002.

[14] H. Weller, G. Tabor, H. Jasak, and C. Fureby, "A tensorial approach to cfd using object oriented techniques," *Comp in Phys.*, vol. 12, pp. 620–631, 1998.
[15] F. R. Menter, M. Kuntz, and R. Langtry, "Ten years of industrial experience with the sst turbulence model," *Proc. Int. Symp. Turbul. Heat Mass Transf.*, vol. 4, pp. 625–633, 2003.
[16] T. Sarpkaya, *Wave Forces on Offshore Structures*. Cambridge University Press: Cambridge, UK., 2014.